Journal of Industrial and Engineering Chemistry 64 (2018) 173–187

Contents lists available at ScienceDirect

Journal of Industrial and Engineering Chemistry

journal homepage: www.elsevier.com/locate/jiec

Adsorption performance of 5A molecular sieve zeolite in water vapor–binary gas environment: Experimental and modeling evaluation

Firas A. AbdulKareem[a], Azmi Mohd. Shariff[a,*], Sami Ullah[a], Tan Lian See[b], Lau Kok Keong[a], Nurhayati Mellon[a]

[a] CO2 Research Center (CO2RES), Chemical Engineering Department, University Teknologi PETRONAS, Sri Iskandar, 32610 Perak, Malaysia
[b] Department of Chemical Process Engineering (CPE), Malaysia – Japan International Institute of Technology (MJIIT), Universiti Teknologi Malaysia (UTM), Jalan Sultan Yahya Petra, 54100 Kuala Lumpur, Malaysia

ARTICLE INFO

Article history:
Received 30 October 2017
Received in revised form 22 January 2018
Accepted 11 March 2018
Available online 17 March 2018

Keywords:
CO_2
Binary and ternary mixtures
Volume–gravimetric analysis
Magnetic suspension balance (MSB)
Artificial neural network (ANN)

ABSTRACT

In this work GERG2008 EoS was incorporated in a volumetric-gravimetric-chromatographic technique. The system utilized to measure in-mixtures components experimental selective isotherms individually, with the ability to analyze water vapor–gas components in the same mixture. 5A zeolite was used as a solid adsorbent for binary and ternary $CO_2/CH_4/H_2O$ mixtures adsorption at 50 °C and 70 °C temperature up to 10 bar pressure. Artificial neural network (ANN) modeling was applied to predict ternary and binary gaseous with the presence of water mixtures. This study delivered better clarification in the field of selectivity and reliability in the term of multicomponent and dual phase mixtures analysis.

Introduction

Carbon dioxide (CO_2) emissions and environmental issues nowadays raise the demands for sophisticated and higher efficiency separation process. More effective separation techniques which related to additional energy consumption need to be investigated and studied, especially in term of highly selective materials innovation. Natural gas and flue gas deliberating the pioneer sources of CO_2 emission [1,2]. Besides, the selectivity of multicomponent mixtures separation studies plays a huge impact on the purification and refining process [3–5].

A typical natural gas composed of a high percentage of methane (CH4), 75%–90%, along with significant amount of other hydrocarbons such as ethane, some propane, butane, and 1%–3% of other higher hydrocarbons [6]. However, according to Darman and Harun [7], the composition of natural gas reserves yields another trend in some Asian Pacific regions, as the CO_2 content in some fields ranges from 30 to 90% at high CO_2 content reserve region. For the intention for natural gas purification [8–11], a variety of selective separation techniques have been considered, and other multi components streams persisted practically, focusing on modeling and theoretical selectivity analysis [12–15]. Adsorption with solid desiccants is as one of the suitable techniques for multi-component mixtures separation and purification processing [16,17]. As such, this work focuses on adsorption-based separation, as it is illustrated more easiness of handling as opposed to liquid solvents and more eco-friendly [18–20].

Several researches were performed for studying binary, ternary, and higher components mixtures selectivity analysis [21–23] on diverse sorts of solid desiccants [24–28] and operating conditions. On theoretical prediction study, most studies focused on the theoretical prediction of selectivity from the results obtained by the pure component adsorption [29]. Henry's law constant, Langmuir model constant for selectivity identification, Ideal Adsorption Solution Theory (IAST) and Real Adsorption Solution Theory (RAST) model [30,31] are some cases of theoretical models utilized for mixture predictions from pure components adsorption data. However, artificial neural network (ANN) concerned excessive attraction and deliberated as a consistent technique compared to other known theoretical models. ANN utilized for the prediction of density, surface tension, and viscosity of components and various mixtures [32–34]. Back-propagation artificial neural network (BP-ANN) model was successfully applied for the simultaneous estimation of vapor–liquid equilibrium (VLE) of four binary systems [35]. While, Fotoohi et al. [36] investigated the capability to predict binary mixtures from aforementioned reported data in the literatures utilizing (2-D EoS) i.e. Redlich–Kwong (RK), Soave–Redlich–Kwong (SRK), Peng–Robinson (PR), and Modified

* Corresponding author.
E-mail address: azmish@utp.edu.my (A. Mohd. Shariff).

https://doi.org/10.1016/j.jiec.2018.03.014
1226-086X/

Mohsennia–Modarress–Mansoori (M4), compared with the data predicted utilizing ANN predictions. However, they claimed that the binary mixtures predicted utilizing ANN model showed better agreement and precision compared to the EoSs mentioned and studied [37,38]. Thus far, there are very few reports in the literature with experimental data regarding multi-component mixtures selective adsorption isotherms representing individual components uptake independently, especially if the mixtures reflecting more than one phase i.e. gases and water vapors.

The ratio of SiO_2/AlO_2 has high impact in the multicomponent mixtures selective separation, which related to the water vapor–solid interaction on ionic solid adsorbents. This might affect the hydrophobicity of the solid adsorbents and in conclusion, negatively affect the adsorption capacity and selectivity. Rana et al. [39] reported that the adhesion forces are an exponential function of macro scale water contact and surface energy due to strong liquid–solid or vapor–solid interaction elaborated in capillary forces. These interactions are subjected to electrostatic-dipole–dipole interaction (hydrogen bonding) on the surface and/or few atomic water layers above the surface. Meanwhile, Kumar and Chowdhury [40] reported that the relatively high selectivity for nitriles on H-USY type zeolites with a high SiO_2/Al_2O_3 ratio might be related to their hydrophobicity, as the hydrophobic H-USY samples could not retain sufficient H_2O.

Zeolite has been reported as a significant material in the application of catalysis, absorption, and ion-exchanging due to their microporous structure [41]. The most commonly used zeolite is Faujasite (FAU) type adsorbents whereby the framework is composed of AlO_4 and SiO_4 tetrahedron. It can also be viewed as SiO_2 with some SiO_4 tetrahedron substituted by AlO_4, resulting in electronegativity of the framework. It can be balanced by the cations attaching to the framework in the pores, such as Na^+, K^+, Mg^{2+}, Ca^{2+}, NH^{4+}, etc. These cations are always easy to be exchanged with external ions. The number and sites of the cations strongly affect the properties of the zeolites.

In this study, 5A molecular sieve zeolite (MSZ) is used as the solid adsorbent since it has high adsorption capacity for pure CO_2 and water (H_2O) compared to silica gel. Although adsorption of gas using 5A MSZ had been studied, previous works by other researchers studied the premixed multi-component mixtures effect by variation of compositions on the total mixture uptake, without further studying the individual uptake of components independently within the mixture.

In this work, a novel setup compared to previously existed techniques [42–44], with the high throughput mathematical approach and EOSs implemented will be presented. CO_2, CH_4, and water vapor combination, as in binary and ternary mixtures were studied for their individual selective isotherms at various predetermined compositions and initial loadings.

This new measurement technique will give the opportunity to compare the pure adsorption of CO_2 and its isotherm modeling with selective CO_2 adsorption within the binary mixture of CO_2: CH_4 in the presence of water vapor. This state of art method contributed a better understanding of the behavior of CO_2 within the binary/ternary mixture, especially with various compositions. In addition, it gives the opportunities to study the manipulations of individual components of the loading compositions and its impact on the total mixture uptake in vapor–gas combinations.

Materials and methods

Materials

5A zeolites molecular sieve beads (Sigma Aldrich, Germany) with the linear formula: 0.80 CaO: 0.20 Na_2O: 1 Al_2O_3: 2.0 ± 0.1 SiO_2: x H_2O was utilized as solid adsorbents in this study. Its physical characteristics consisted of BET surface area ≈538.47 $m^2\,g^{-1}$, pore d_m ≈2.101 nm and pore volume ≈0.303 $cm^3\,g^{-1}$. Helium (He) (99.999%), CO_2 (99.995%) and CH_4 (99.995%) were purchased from Linde Sdn. Bhd., Malaysia. Distilled water was used for water vapor generation.

Experimental setup

The adsorption measurements were performed in the custom designed volume-gravimetric system from Rubotherm GmbH., Germany. Fig. 1 demonstrates the main parts and sections of the

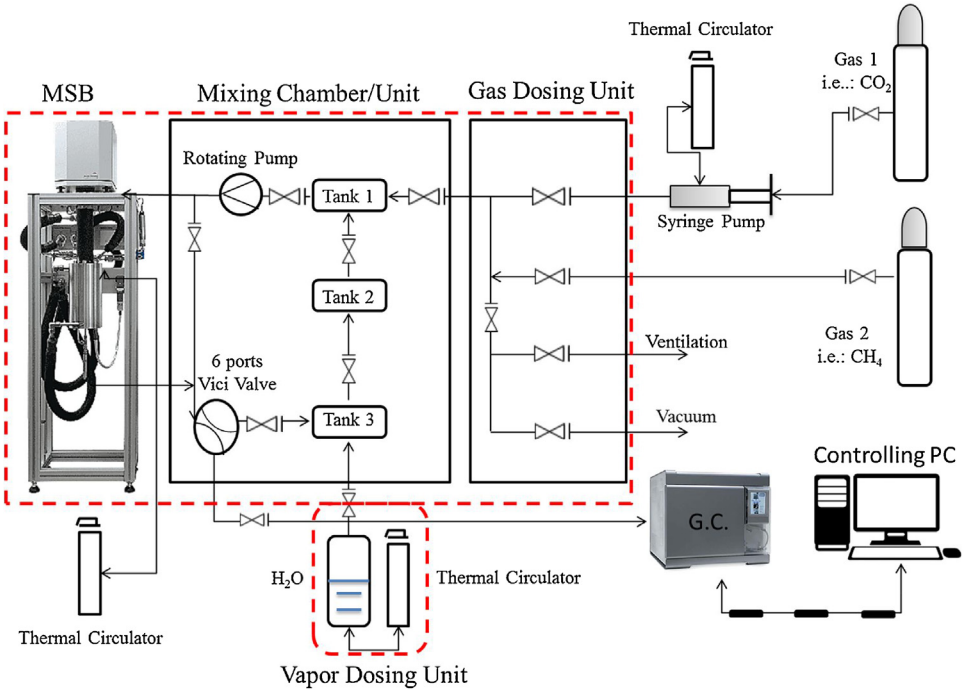

Fig. 1. Schematic diagram of the volumetric-gravimetric experimental system.

experimental setup. The dosing system is responsible for gases and vapor dosing to the mixing chamber, while the mixing chamber/unit (MC) is responsible for mixing the adsorbates and created a homogeneous mixture before expanded to the reaction chamber/cell (RC). The RC consisted of magnetic suspension balance (MSB) and it was connected to the custom-made Danni-Master Gas Chromatograph (GC). The custom-made Dani Master GC was controlled by the Clarity software and equipped with a thermal conductivity detector (TCD), Split/Split-less injector, and custom made (HayeSepQ, 3 m, 1 mm, 1/16", 80/100 mesh PC11518) column. The GC was utilized to determine the actual composition of the gas/vapor binary and ternary combinations before and after adsorption process. The high accuracy MSB was used to measure the change in mass and density of the sample of material and gases, respectively. The GC was equipped with a thermal conductivity detector (TCD), Split/Split-less injector, and custom made (HayeSepQ, 3 m, 1 mm, 1/16", 80/100 mesh PC11518) column to identify the actual composition of the mixture in the mixing unit before expansion to the reaction chamber. Multipoint gases and vapors GC calibrations were performed whenever a new combination of gases was utilized.

Blank and buoyancy calibrations

In the blank measurement, inert gas i.e.: He was utilized to measure the sample basket weight and volume of empty sample cell (without sample) at the same operating temperature and pressure. Fig. 2 shows the forces were exerted during blank measurements and properties measured by balance, represented by Δm as corrected mass Eqs. (1)–(4). The force, F_B is the buoyancy force upward and F_A is the adsorption force or the gravimetric force according to the adsorbed mass of solute (gas). V^{sc} is the volume of the sample basket and m^{sc} is the mass of the sample basket.

$$F_B = V^{sc}.\rho(P,T,y).g \tag{1}$$

$$F_A = m^{sc}.g \tag{2}$$

$$F_{EXP.} = F_A - F_B = g.(m^{sc} - V^{sc}.\rho(P,T,y)) \tag{3}$$

$$\Delta m = \frac{F_{EXP.}}{g} = (m^{sc} - V^{sc}.\rho(P,T,y)) \tag{4}$$

Blank measurement usually consisted around 6–8 segments with the first segment carried out under a vacuum condition to identify the density of gas equivalent to zero (r = 0). The sample cell weight equivalent to the mass acquired by the balance reading at the zero-point pressure. The volume of the sample basket reduced to zero at vacuum condition as indicated by Eqs. (4) and (5):

$$\Delta m = m^{sc} \tag{5}$$

The blank measurement was conducted to determine the initial adsorbent holder/basket mass and volume prior adsorption, as these values were essential in further calculations and balance tarring in case a balance drifting occur during measurements [45].

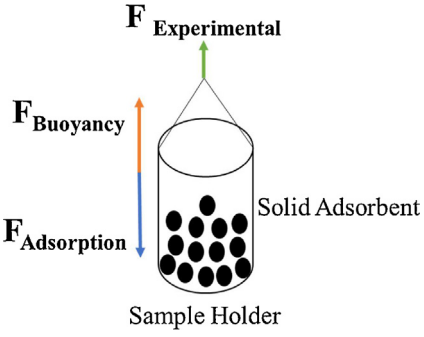

Fig. 2. Forces exerted on the sample basket cell during adsorption measurements and balance reading.

Buoyancy measurements

For a precise pressurized gravimetric measurement, the correction of buoyancy force was incorporated. Eqs. (6)–(8) demonstrated the forces exerted on the sample during buoyancy effect and the parameters which were taken into consideration [46,47].

$$F_B = (V^{sc} + V^s).\rho(P,T,y).g \tag{6}$$

$$F_A = (m^{sc} + m^s).g \tag{7}$$

$$F_{EXP.} = F_A - F_B = g.(m^{sc} + m^s - (V^{sc} + V^s).\rho(P,T,y)) \tag{8}$$

where F_A, F_B, and F_{EXP} are adsorption gravimetric force, buoyancy force and balance reading force, respectively. Eqs. (9) and (10) were used for calculation of sample mass and sample volume during buoyancy measurement.

$$\Delta m = \frac{F_{EXP.}}{g} = m^{sc} + m^s - (V^{sc} + V^s).\rho(P,T,y) \tag{9}$$

$$\Delta m = m^{sc} + m^s \tag{10}$$

As the blank measurement was considered $(m^{sc}+m^s)$ and $(V^{sc}+V^s)$, as m^s and V^s are sample mass and sample volume, respectively. While in the blank measurement m^{sc} and V^{sc} illustrated by the difference between the two outcomes and the values of m^s and V^s was measured. From this, the sample density r^s was identified. Since m^s did not take into consideration the small amount of inert gas adsorbed, the corrected mass m^s needs to be calculated by using Eq. (11) [45]:

$$m^{scorr.} = \Delta m^{at\ vac.} - m^{sc} \tag{11}$$

where $\Delta m^{at\ vac}$ is the first segment reading of the balance at vacuum. In this equation, the amount of inert gas adsorbed during the buoyancy measurement for further accuracy and concerns. Blank and buoyancy measurements were carried out whenever the thermal operational conditions of the experiments changed or the sample was exposed to the enviroment, where the mass and volume of the sample might be effected by adsorbed air and humidity [48].

Samples pretreatment and regeneration

Prior to each adsorption experiment, the adsorbent was pretreated using an electrical heater along with the thermal bath circulator. Pretreatment process was crucial to get rid of contaminants and moisture trapped in the adsorbent pores and cavities, using electrical heater under vacuum condition. According to Tedds et al. [49], 200–250 °C of thermal treatment was regarded as the best range for samples pretreatment and degassing/regeneration. However, based on our thermal gravimetric analysis (TGA) results, zeolites lost moisture and contaminants at around 200 °C and sample did not decompose until 800 °C. Therefore, in this work, pretreatment and regeneration of the adsorbent was

carried out at a temperature of 200 °C for at least 3 h until sample weight decrease had stabilized.

Adsorption measurement

Adsorption equilibrium of pure gases was performed in a magnetic suspension microbalance operated in a closed system. After samples were pretreated and regenerated, gases were dosed via into the reaction chamber directly. The sample of adsorbent was weighed and placed in a basket suspended by a permanent magnet through an electromagnet (magnetic suspension coupling). The cell in which the basket was housed was then closed, and vacuum was applied. An analytical balance connected to the magnetic coupling receives the weight values measured inside the cell, and through an acquisition system, records the data in system software [37,50]. The magnetic suspension balance utilized in this study was equipped with microbalance i.e.: 10^{-6} precision, 0.01 mg resolution, <0.002% rdg uncertainty, and 0.04 mg reproducibility/standard deviation). The balance readings were collected at equilibrium for each segment and processed for further analysis. The individual adsorbates and total mixture densities were identified by the material balance and GERG2008 EoS. GERG 2008 [51] covers most of the natural gas components and contaminants with a comprehensive assortment of working conditions.

Multicomponent experimental adsorption

The water vapor–gas mixtures expressive advanced challenging process to be initialized and evaluated. Water vapors are complicated to be generated and dosed at vapor partial pressure at liquid boiling points and premixed with gases at higher partial pressures, to cater the mixture total pressure with avoided condensation, especially at higher vapors concentration or compositions demanded. In addition, limited dual phase identification and analysis instrumentation recently existed.

In the water vapor–gas mixtures measurements, the experiments took place by premixing the dosed gases with generated water vapor at fixed combinations (99:1 gas/vapor). Then, individual components were dosed accordingly at certain gas and vapor pressures to cater for the determined compositions for each particular isotherm point. This generation and mixing technique would provide better accuracy outcomes for the data collected before and after adsorption.

In multicomponent mixtures, three mixture configurations were studied to determine the effect of CO_2, CH_4 and water vapor (if any) presence in the mixture on the 5A molecular sieve zeolite adsorption capacity and selectivity. The mixtures were considered to cover a wide range of multi-component applications i.e. CO_2:CH_4; CO_2:H_2O; CH_4:H_2O; premixed CO_2:CH_4:H_2O and CO_2:CH_4 with preloaded H_2O. The ratio binary component of CO_2:CH_4 was fixed at 50:50, 30:70 and 70:30 while the ratio of H_2O, if present in the mixture, was fixed at 1%. In preloaded water vapor measurements, the samples were preloaded with pure water vapor at the same amount that was dosed as in the ternary premixed measurements to achieve the same percentage dosed in the premixed ternary mixtures i.e.: 1% water vapor. The measurements were performed at the conditions of 50 °C and 70 °C and the pressure was varied up to 10 bar.

The measurement for partial uptakes of each component in the mixture was determined by calculating the adsorbed amount of each component into the mixture independently with the aid of GERG2008 EoS. The GERG2008 equation of state was based on a multi-fluid approximation explicit in the reduced Helmholtz free energy as deliberated in Eq. (12):

$$a(\delta.\tau.\bar{x}) = a^o(\rho.T.\bar{x}) + a^r(\delta.\tau.\bar{x}) \tag{12}$$

where the a^o represented the properties of the ideal-gas mixture at a given mixture density r, temperature T, and molar composition $\bar{x}$ as mentioned in Eqs. (13) and (14):

$$a^o(\rho.T.\bar{x}) = \sum_{i=1}^{N} x_i \left[a^o_{oi}(\rho.T) + \ln x_i\right] \tag{13}$$

The residual part a^r of the reduced Helmholtz free energy of the mixture is given by Eq. (14):

$$a^r(\delta.\tau.\bar{x}) = \sum_{i=1}^{N} x_i a^r_{oi}(\delta,\tau) + \sum_{i=1}^{N-1}\sum_{j=i+1}^{N} x_i x_j F_{ij} a^r_{ij}(\delta,\tau) \tag{14}$$

where δ is the reduced mixture density and τ is the inverse reduced mixture temperature according to Eq. (15):

$$\delta = \frac{\rho}{\rho_r(\bar{x})} \quad \text{and} \quad \tau = \frac{T_r(\bar{x})}{T} \tag{15}$$

where N represented the total number of components. Detailed numerical descriptions of single and multicomponent mixtures measurements and thermodynamic properties, which presented using GERG2008 EoS were discussed in a study by Kunz and Wanger [51].

Equilibrium isotherm models

Extended Langmuir (EL) model

Extended Langmuir model was used to model the adsorption equilibrium data in the binary system of CO_2/CH_4 mixtures at different concentrations (i.e. 50:50, 30:70, and 70:30) based on single component data. The mathematical expression of extended Langmuir model is given in Eq. (16):

$$q_{e,i} = \frac{q_{m,i} K_i P_{e,i}}{1 + \sum_{j=1}^{n} K_i P_{e,i}} \tag{16}$$

where $q_{e,i}$ is the uptake of component i, q_m and K_i in Eq. (16), are Langmuir constants for maximum adsorption capacity of the adsorbents (mg/g) and absorptivity of the adsorbates (bar/mg) in a single system, respectively.

$$q_{e,1} = \frac{q_{m,1}.K_{L,1}.P_{e,1}}{1 + K_{L,1}.P_{e,1} + K_{L,2}.P_{e,2}} \tag{17}$$

$$q_{e,2} = \frac{q_{m,2}.K_{L,2}.P_{e,2}}{1 + K_{L,1}.P_{e,1} + K_{L,2}.P_{e,2}} \tag{18}$$

where q_m and K_L in Eqs. (17) and (18) are Langmuir constants for maximum adsorption capacity of the adsorbents (mmol/g) and adsorptivity of the adsorbates in a single system, respectively [52].

The applications of extended Langmuir model to represent adsorption equilibrium data in the binary system were reported in several studies [53,54]. From the previous studies, it was known that the evaluation of binary adsorption equilibrium data using extended Langmuir model was performed by inserting the values of q_m and K_i parameters in a single system to calculate the theoretical value of q_e and compared it with experimental results. Extended Langmuir model was applied on CO_2 and CH_4 single adsorption data that fitted to Langmuir equilibrium isotherm model. Langmuir constant and single component maximum adsorption capacity at experimental operational conditions were applied and analyzed accordingly.

Modified Extended Langmuir (MEL) model

In a binary system, the competitions (total or partial) between adsorbate species for the adsorption sites on the solid surface

usually occur, which may act as the sorption-controlling factor. Such phenomena result in the coverage of the solid surface by both adsorbates with certain fractional loadings. Moreover, the adsorption potential on the surface is also affected by lateral interaction or competition between adsorbate species in the system. From the statements above, it is obvious that both K_i and q_m parameters from single Langmuir model cannot be adequately used to describe adsorption behaviors in a binary system. Therefore, Kurniawan et al. [52] were proposed an improved mathematical equation for q_m and K_i parameters for binary adsorption system, which is given in following Eqs. (19)–(21):

$$q_{m(binary)} = q_{m,1(\text{single})}\theta_1 + q_{m,2(\text{single})}\theta_2 \tag{19}$$

$$K_{1,(binary)} = K_{1(\text{single})}\exp\left(\frac{-\theta_2}{\theta_1}\right) \tag{20}$$

$$K_{2,(binary)} = K_{2(single)}exp\left(\frac{-\theta_1}{\theta_2}\right) \tag{21}$$

where, θ_1 and θ_2 are loading fraction of component 1 and 2, respectively. Following this technique will enable the effect of the initial composition studied of the binary mixture to be visibly observed in addition to the intensity effect. This wi correct the ideality behavior deviations that might highly affect the outcomes of the theoretical model and predictions. Lastly, the amount adsorbed for the binary mixture is described by Eqs. (22) and (23), Langmuir constant from single adsorption data was utilized. In addition, the molar fraction required to be studied for the particular configuration of the mixture was considered.

$$q_{e,1(bin)} = \frac{\left(q_{m,1(\text{sing})}\theta_1 + q_{m,2(sing)}\theta_2\right)K_{L,1(sing)}\exp\left(\frac{-\theta_1}{\theta_2}\right)C_{e,1(bin)}}{1 + K_{L,1(sing)}\exp\left(\frac{-\theta_2}{\theta_1}\right)C_{e,1(bin)} + K_{L,2(sing)}\exp\left(\frac{-\theta_1}{\theta_2}\right)C_{e,2(bin)}} \tag{22}$$

$$q_{e,2(bin)} = \frac{\left(q_{m,1(\text{sing})}\theta_1 + q_{m,2(sing)}\theta_2\right)K_{L,2(sing)}\exp\left(\frac{-\theta_1}{\theta_2}\right)C_{e,2(bin)}}{1 + K_{L,1(sing)}\exp\left(\frac{-\theta_2}{\theta_1}\right)C_{e,1(bin)} + K_{L,2(sing)}\exp\left(\frac{-\theta_1}{\theta_2}\right)C_{e,2(bin)}}. \tag{23}$$

The model applied to pure adsorption data of single CO_2 and CH_4 was also utilized to predict binary CO_2/CH_4 mixtures at different configurations (i.e. 50:50, 30:70, and 70:30). The outcome would be compared with the binary gaseous mixture data from experimental results. This will give a better idea whether the model could improve the predicted adsorption trend by taking considerations the polar moment and polarizability of single component affinity for adsorption and selectivity in binary mixtures.

Artificial neural networks (ANN)

In this study, the ANN architecture as illustrated in Fig. 3a was selected as a feedforward ANN with two hidden layers consisting of 12 and 8 neurons for binary gases mixtures with preloaded water vapor. The number of hidden neurons tested to achieve the lower mean square error (MSE) is illustrated in Fig. 3b. Twelve (12) hidden neurons were selected in the case of ternary mixtures as MSE showed the lowest value which was the closest to zero compared to the other 20 hidden neurons tested. The 5 input variables are temperature, pressure, CO_2, CH_4, H_2O i.e. in ternary mixtures, and total mixture uptakes, and the 4 output variables are CO_2, CH_4, H_2O and Mixture uptakes. The set of experimental data was divided into three groups. Around 70% of the experimental

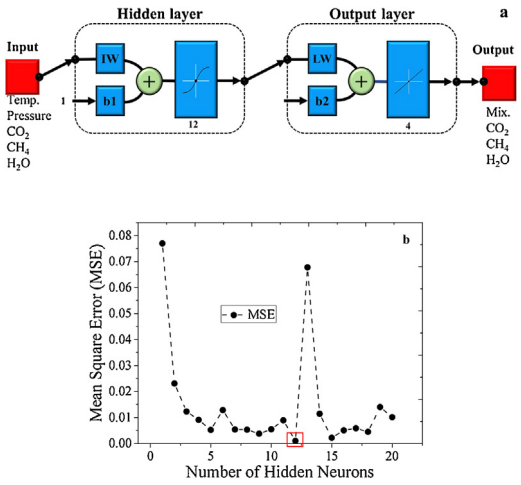

Fig. 3. Artificial neural network function (feed-forward ANN) (a) design generated from MATLAB (b) the number of hidden neurons tested for minimum mean square error (MSE) value.

data was used for the training step, 15% for testing and other 15% for validation [55]. The training function selected for this step is known as trainlm. Trainlm is a widely used training function as it updates the results according to Levenberg–Marquardt optimization method. The results from the ANN modeling are discussed in the results and discussion section.

Results and discussions

Verification of adsorption performance

Before the measurement of adsorption in binary gas and water vapor–binary gas environment was conducted, the adsorption of single gas (CO_2 and CH_4) on 5A zeolite at 50 °C and 70 °C and pressure up to 10 bar was measured and compared with previously reported data by Mofarahi et al. [56]. In this work, CO_2 adsorption on 5A MSZ showed higher adsorption 4.05 mmol/g compared to 1.23 mmol/g for CH_4 at 50 °C. Lower adsorption uptakes were observed for both adsorbates at 70 °C. The adsorption of CO_2 was 3.06 mmol/g and 1.21 mmol/g for CH_4. Fig. 4 shows the comparison of measured data obtained in this work and literature data. In general, the measured data in this work is quite close to the literature data. The slight difference in the measured data between these two works could be due to the different experimental setup employed whereby Mofarahi et al. [56] measured the adsorption based on volumetric setup while the measurement in this work was based on volumetric-gravimetric setup.

Equilibrium isotherm models for CO_2 and CH_4

Two and three parameters isotherm models, namely Langmuir, Freundlich, Sips, and Toth was conducted for pure gas adsorption data for validation and analysis of CO_2 and CH_4 adsorption behavior. Fig. 5 illustrates the isotherm models fitting on CO_2 and CH_4 experimental data at a temperature of 50 °C and 70 °C and pressure up to 10 bar. The results show high agreement for most of the isotherm models. Langmuir and Toth equilibrium isotherm models showed the highest fitting for CO_2 adsorption experimental data on 5A MSZ while Freundlich isotherm model showed the lowest agreement ($r^2 = 0.886$) with the experimental data as given in Table 1.

Adsorption of CH_4 on 5A zeolite showed almost linear uptake as shown in Fig. 5. The equilibrium isotherm parameters for CH_4 uptake on 5A zeolite at a temperature of 50 °C and 70 °C, as listed in

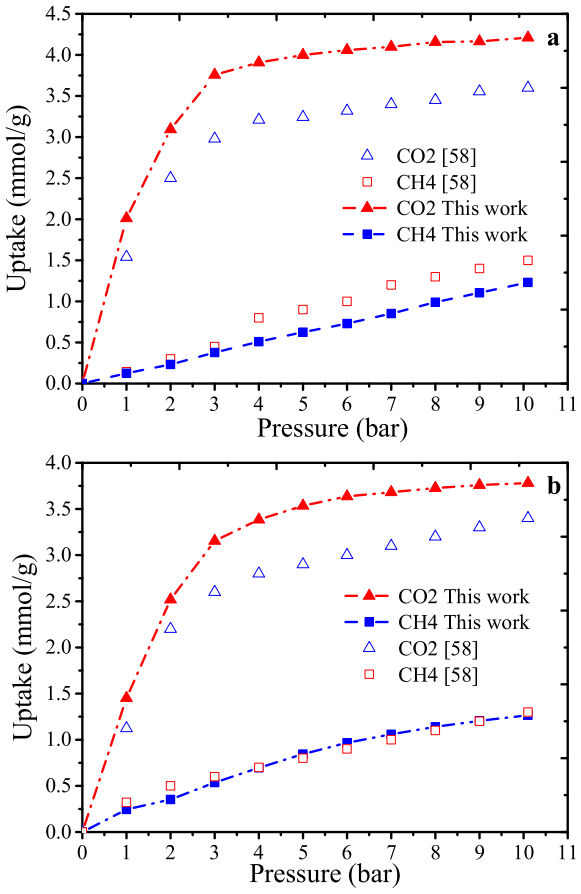

Fig. 4. Pure CO_2/CH_4 components adsorption on 5A MSZ at temperature of (a) 50 °C and (b) 70 °C at increment pressure up to 10 bar.

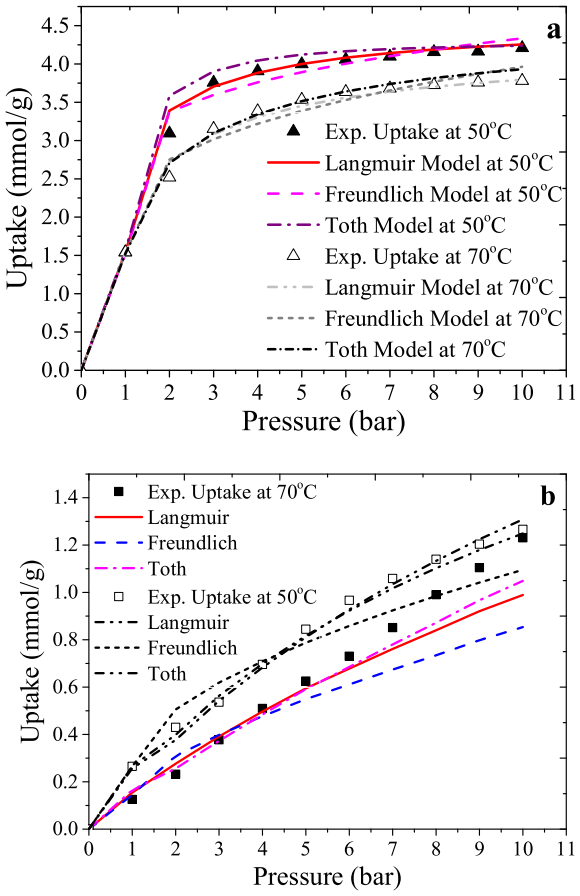

Fig. 5. Equilibrium isotherm models for (a) CO_2 and (b) CH_4 adsorption on 5A zeolite at 50 °C and 70 °C temperature and up to10 bar pressure.

Table 2 showed that the experimental data were in agreement with Langmuir, and Toth equilibrium isotherm models. Equilibrium parameters showed that monolayer adsorption is the most common behavior illustrated in CH_4 adsorption on 5A with high Langmuir agreement. Freundlich Equilibrium model showed lower agreement with the experimental data compared to the other equilibrium models which were clarified according to the values of R^2. However, Freundlich isotherm model constant deliberated a value more than 1, which is a supported physical adsorption behavior. The validation of the equilibrium characteristics obtained from the equilibrium isotherm models provided the opportunity to apply the equilibrium models parameters for binary mixtures theoretical predictions.

Experiment and model evaluation for binary and ternary component measurements

Binary gas mixtures

In this work, three different compositions were studied for CO_2:CH_4, to identify the deviation effect in multi-components existences by identifying initial compositions on the selective adsorption of individual gases and the total uptake of the mixture. The results of the binary gaseous mixtures adsorption on 5A zeolite are presented in the Fig. 6. The results verified the whole mixture gravimetric uptake, with the individual isotherms of each component inside the mixture experimentally, which deliberated the novelty of this work.

The results show that CO_2 has the higher potential for adsorption on 5A zeolite. CO_2 has the highest affinity due to its strong quadrupole moment [57], while lower potential presented for CH_4. Furthermore, at different CO_2 compositions, the whole mixture uptake was affected. As shown in Table 3, the total gravimetric uptake of the whole mixture increased with the higher CO_2 composition at 70% compared to 50 and 30% CO_2. In addition, CO_2 still expressed higher adsorption uptake independently even at lower compositions as in the 30:70 CO_2:CH_4 mixture.

Table 1
Adsorption equilibrium isotherm parameters for CO_2 adsorption on 5A MSZ at 323 K and 10 bar.

	Isothermal parameters							
	Adsorption at 323 K				Adsorption at 343 K			
5A/CO_2	R^2	K	q_m	n	R^2	K	q_m	n
Langmuir	0.999	1.219	4.564	/	0.999	0.915	4.358	/
Freundlich	0.741	151.774	4.658	13.568	0.886	103.490	4.589	4.411
Toth	0.999	0.243	4.679	0.555	0.996	0.892	4.657	1.110

Table 2
Adsorption equilibrium isotherm parameters for CH_4 adsorption on 5A MSZ at 323 K and 10 bars.

	Isothermal parameters							
	Adsorption at 323 K				Adsorption at 343 K			
5A/CH_4	R^2	K	q_m	n	R^2	K	q_m	n
Langmuir	0.989	0.062	1.658	/	0.989	0.989	1.356	/
Freundlich	0.851	3.077	1.786	1.549	0.851	0.851	1.451	2.069
Toth	0.999	0.045	1.596	0.662	0.999	0.999	1.438	0.999

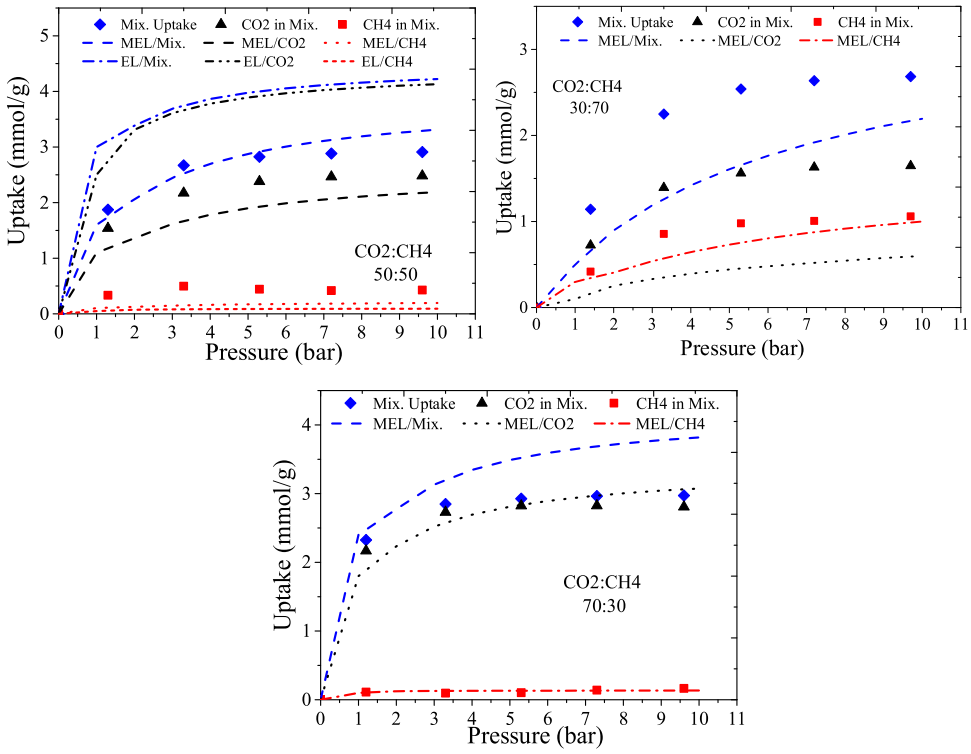

Fig. 6. Experimental and predicted by EL and MEL models binary CO_2:CH_4 mixtures on 5A zeolite at 50 °C temperature and up to 10 bar pressure.

Table 3
Experimental binary gases CO_2:CH_4 mixture total and partial uptakes on 5A MSZ.

Uptakes at 50 °C (mmol/g)			
Configuration	30:70	50:50	70:30
Total mixture	2.684	2.909	2.971
CO_2	1.647	2.481	2.806
CH_4	1.059	0.428	0.164
Uptakes at 70 °C (mmol/g)			
Configuration	30:70	50:50	70:30
Total mixture	2.412	2.656	2.767
CO_2	1.482	2.297	2.669
CH_4	0.930	0.358	0.1439

This experimental selective adsorption behavior of CO_2 on 5A zeolite compared to the potential adsorption of CH_4 are validated with the theoretical selectivity analysis performed by the previous researchers as mentioned earlier and the pure measurements were done in this study. These outcomes were in agreement with the aforementioned reported data at nearby conditions for the adsorption of CO_2 and CH_4 on zeolites other microporous solid adsorbents [30,58].

EL model was applied to estimate binary CO_2:CH_4 mixtures according to the individual components adsorption experimental data. The outcomes were linked with the experimental multicomponent binary and ternary measurements achieved by the volumetric-gravimetric method at the same operational conditions of the pure component measurements.

Fig. 6 displays the predicted binary combinations by EL model and its comparison with experimental data of binary mixtures i.e. CO_2 and CH_4 at same compositions. From the figure, it is observed that the predicted binary mixtures followed the ideal selectivites of the pure adsorption. Irrespective the attraction to adsorb distinct components within the binary mixture, as quadrupole moment and polarizability of CO_2 is higher than CH_4. This leads to the inference that 5A has the potential to adsorb CO_2 if competing with CH_4, despite the configuration of the individual components in the mixture.

However, the predicted amount of CO_2 in the binary mixture at 50 °C was almost the same with a very low decline in values compared to pure CO_2 component adsorption data, which is not reflected the best prediction that can be relied on. In the case of binary mixture predicted on 5A MSZ at 70 °C, the pure CO_2 components adsorption data illustrated higher values compared to predicted fractions in the mixture for both components. On the other hand, the results acknowledged the temperature effect on the adsorption process where the results obtained by the EL at 70 °C were lower in general compared to the first case i.e. at 50 °C. However, this behavior reflects the flow dependence on the pure adsorption data. The EL prediction is still limited and totally relied on the experimental data obtained by the pure component outcomes and cannot be extended for further predictions at other configurations as perceived in MEL model.

Similarly, Modified Extended Langmuir (MEL) model was applied to predict the adsorption outcome to evaluate its suitability compared to the EL model. The outcomes of binary gaseous CO_2:CH_4 mixtures on 5A MSZ at the studied configuration i.e. 30:70, 50:50, and 70:30 CO_2:CH_4 mixtures at a temperature of 50 °C and 70 °C, and pressure up to 10 bar are illustrated in Figs. 6 and 7. MEL model exhibited an altered behavior compared to EL model. CO_2 uptake in EL model showed higher partial uptakes as compared to CH_4, even with advanced values of initial CH_4 configurations in the mixture.

However, in the MEL model, at 50 °C, the situations were different, as the anticipated mixture followed the fractional loading parameter of the two components, which presented the amount of each element existing into the mixture. With higher presence of CO_2 in the mixture 70% y_{CO_2}, the predicted quantity adsorbed of CH_4 was practically very low at 2.72 mmol/g CO_2, compared to 0.14 mmol/g CH_4. This is highly denoted by the

quadrupole moment and polarizability of CO_2, which is highly associated to CH_4. This increases the potential of 5A zeolite to adsorb more CO_2 to CH_4 at the mixture, despite the composition of the distinct adsorbates.

Further increase in the CH_4 mixture composition led to decrease in CO_2 predicted uptakes, as demonstrated in 50:50 arrangements. When the CO_2 concentration was decreased from 70% to 50%, the predicted CO_2 uptake at 50 °C decreased from 2.72 mmol/g CO_2 to 1.71 mmol/g. On the other hand, the predicted CH_4 uptake increased from 0.13 to 0.31 mmol/g as its concentration was increased from 30% to 50%. These outcomes are closer to the measured experimental data as compared to the data predicted from MEL model. As CH_4 concentration increases in the mixture, the competition among CH_4 and CO_2 on occupying 5A zeolite's pores would increase as well. Even though CO_2 has more affinity and potential to be adsorbed over CH_4, CO_2 adsorption still can be affected by the presence of huge amount of CH_4. Thus, this high percentage of CH_4 existence in the mixture will not only increase the competition but also creates a hindrance for CO_2 to be adsorbed easily on 5A MSZ surface.

The effect of increasing the concentration of CH_4 in the mixture is clearly shown in CO_2:CH_4 mixtures at the composition of 30:70. CO_2 uptake was significantly decreased down to 0.51 mmol/g when its concentration was decreased from 70% to 30%. At the same time, CH_4 uptake was increased up to 0.92 mmol/g as compared to 30% CH_4 existence at the same operational conditions.

Fig. 7 was demonstrated the results of MEL model for CO_2/CH_4 mixtures on 5A MSZ at 70 °C. The results explained the feasible outcomes with the lower total mixture and single components capacities compared to the same configuration on 5A zeolite at the 50 °C case. Although, the predicted CO_2 partial adsorption isotherms showed lower capacities (0.65 mmol/g) compared to CH_4 (0.75 mmol/g) with high methane existence in 30:70 CO_2:CH_4 mixtures.

5A MSZ exposed a favorable potential as a solid adsorbent for separating CO_2 from CH_4 via adsorption. However, for CO_2:CH_4 mixtures predicted at 30:70 configuration, CH_4 showed higher adsorption uptakes in mixture compared to CO_2 which might not be the real case, as CO_2 is known to have higher adsorption affinity as compared to CH_4. According to higher quadrupole moment and polarizability, even with lower compositions availability in the mixture, CO_2 was expected to have higher adsorption capacity and selectivity.

This issue was highlighted by Harlick and Tezel [59] as they observed that the precision of the forecast of CO_2 for different models varies depending on the range of concentration in the gas phase. The EL model predicted CO_2 binary isotherm exactly for CO_2 concentrations higher than 30%. Thus, the model failed to describe the binary mixture at a lower CO_2 concentration (for instance 30% and lower) at relatively low pressures i.e. up to 1 bar. In contrast, the above concentration of components that overlaps the adsorption affinity for single components, which reflects the unreliability of the phenomena that the prediction models rely on. However, the same outputs at higher pressure declared in this study, as MEL model did not describe the system well at lower CO_2 compositions in the mixture.

The outcomes of this section proved that theoretical multicomponent models usually did not provide the optimum method to predict the mixtures behavior on solid adsorbents, as observed from the results of MEL model and EL model although the models were endorsed by several previous studies over IAST and other models. Therefore, under such scenario, trained model such as ANN model could be the alternative option.

Single gas–water vapor mixtures

Figs. 8 and 9 present the adsorption isotherm of premixed binary mixtures of CO_2:H_2O and CH_4:H_2O at 99:1 mixture compositions at 50 °C and 70 °C, respectively. The outcomes clarified that water vapor showed lower selective adsorption of the binary mixtures compared to the other adsorbates, in term of gases uptake. Water vapor existence declines the overall

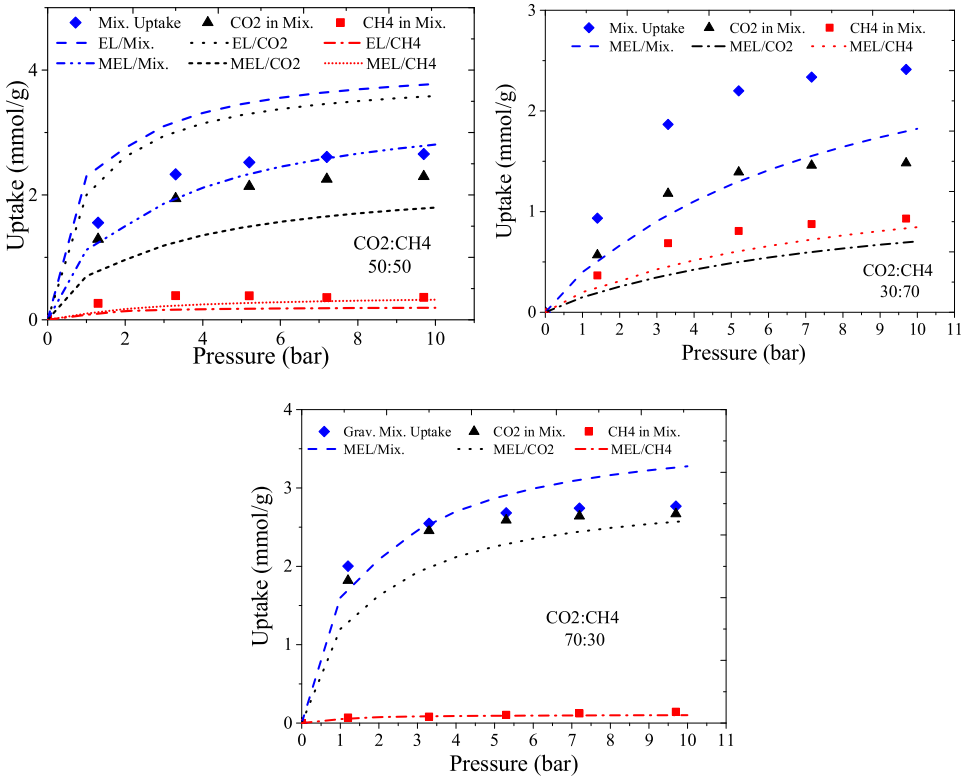

Fig. 7. Experimental and predicted by EL and MEL models binary CO_2:CH_4 mixtures on 5A zeolite at 70 °C temperature and up to 10 bar pressure.

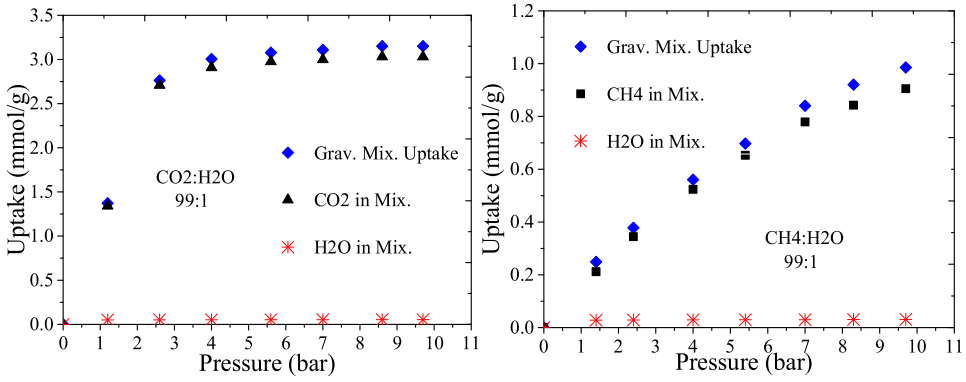

Fig. 8. Single gas–water vapor mixtures of CO_2:H_2O and CH_4:H_2O on 5A MSZ at 323 K and 10 bar.

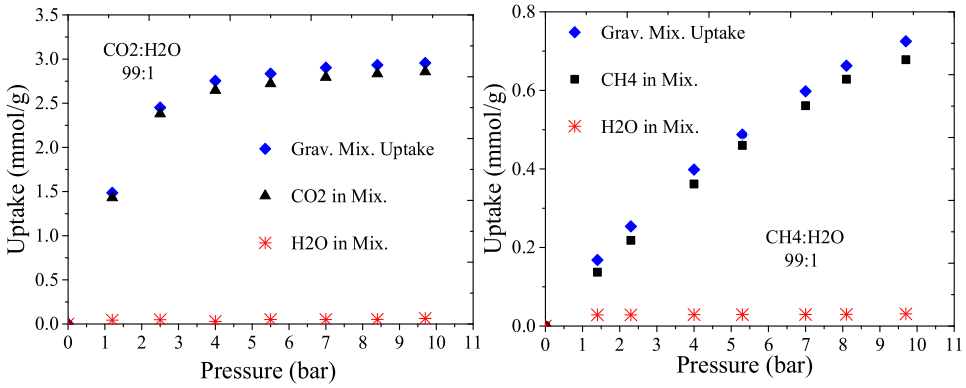

Fig. 9. Single gas–water vapor mixture of CO_2:H_2O and CH_4:H_2O on 5A MSZ at 343 K and 10 bar.

adsorption uptake of the whole mixture, similarly as individual components. Water vapor showed slightly higher adsorption with CO_2 compared to CH_4 binary mixtures. At a temperature of 50 °C, the outcomes showed 0.053 mmol/g for water vapor with CO_2 and 0.030 mmol/g uptake with CH_4, while, at the temperature of 70 °C, water vapor showed 0.062 mmol/g with CO_2 and 0.030 mmol/g with CH_4. These outcomes observed that the adsorption of water vapor was not significantly affected by the adsorption temperature increase compared to the other gaseous adsorbates, and lower adsorption potential for CH_4 compared to CO_2. It might be referred to the phase transitions in natural zeolites and the significance of P_{H2O} that exaggerated the adsorption capacity and selectivity of zeolites, as described by several studies [60,61] while discussed the adsorption of pure CO_2 and binary mixtures of CO_2:H_2O at 0, 25, and 50 °C at ambient pressure. The reported outcomes showed that the increase of water existence will drop the whole binary mixture uptake even under the same conditions, and that might be due to the competition of components or the lower adsorption of the main adsorptive component (for instance CO_2) [62].

Based on Figs. 8 and 9, it is observed that water vapor existence did not affect the uptake isotherm patterns for both adsorbates. Isotherms track the same trends as their pure adsorption isotherm, which almost linear for CH_4 and type I for CO_2 adsorption. However, water vapor presence diminished the adsorption uptake for both CO_2 and CH_4. When there is a trace amount of H_2O in the system, CO_2 and CH_4 adsorption declined by approximately 25% from 4.05 mmol/g and 1.23 mmol/g for pure components adsorption to 3.030 mmol/g CO_2 and 0.905 mmol/g for CH_4 at 50 °C. Almost same drop percentage at the same reduced performance was also observed for adsorption at a temperature of 70 °C, as shown in Table 4, with a trace amount of H_2O as low as 1% of the binary mixture. This might be attributed to the quadrupole momentum (13.71×10^{-40} for CO_2; and 0 for CH_4)

Table 4
Single gas–vapor CO_2:H_2O and CH_4:H_2O mixtures total and partial uptakes on 5A MSZ.

Uptakes at 50 °C (mmol/g)		
Configuration	CO_2:H_2O	CH_4:H_2O
Total mixture	3.150	0.985
CO_2/CH_4	3.030	0.905
H_2O	0.053	0.030
Uptakes at 70 °C (mmol/g)		
Configuration	CO_2:H_2O	CH_4:H_2O
Total mixture	2.955	0.725
CO_2/CH_4	2.857	0.678
H_2O	0.062	0.030

or high degrees of polarizability of $CO_2 \approx 29.1 \times 10^{-25}$ compared to $CH_4 \approx 25.9 \times 10^{-25}$ [53,61]. These outcomes were in agreement with the aforementioned data as CO_2 has the peak quadrupole moment, which monitors in the order $CO_2 > N_2 > O_2 > CH_4$ with values of 13.4, 4.7, 1.3, 0, respectively. However, due to the octupole moment of the methane molecule, CH_4 might show higher equilibrium adsorption capacity of some adsorbents compared to N_2 and O_2 [19].

Binary gas–water vapor mixtures

Figs. 10 and 11 show the total and selective adsorption of the three ternary mixtures configurations at 50 °C and 70 °C, respectively. On top of that, the individual isotherm measured for each component in the mixture, the total amount adsorbed of the three components for each point in the figure will give the whole mixture gravimetric adsorption uptake at the same particular point. Such rehearsal motivation delivered a new field of interest,

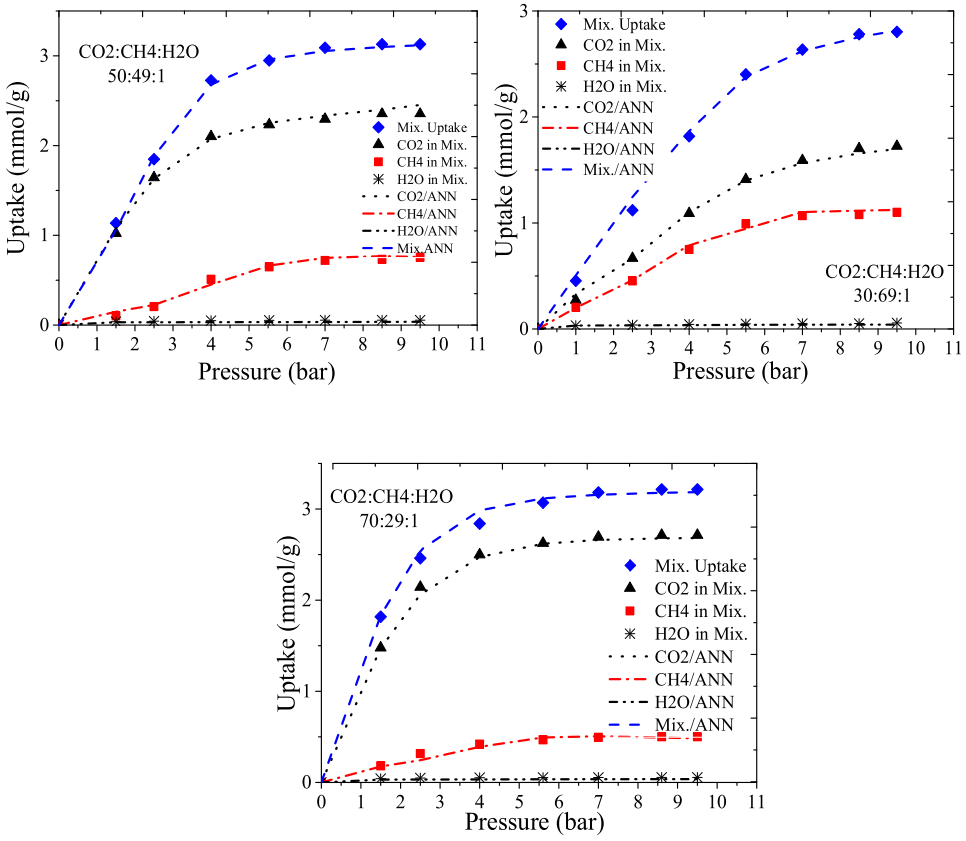

Fig. 10. Ternary CO_2:CH_4:H_2O mixtures total and partial uptakes on 5A zeolite at experimental condition of 50 °C and up to 10 bar.

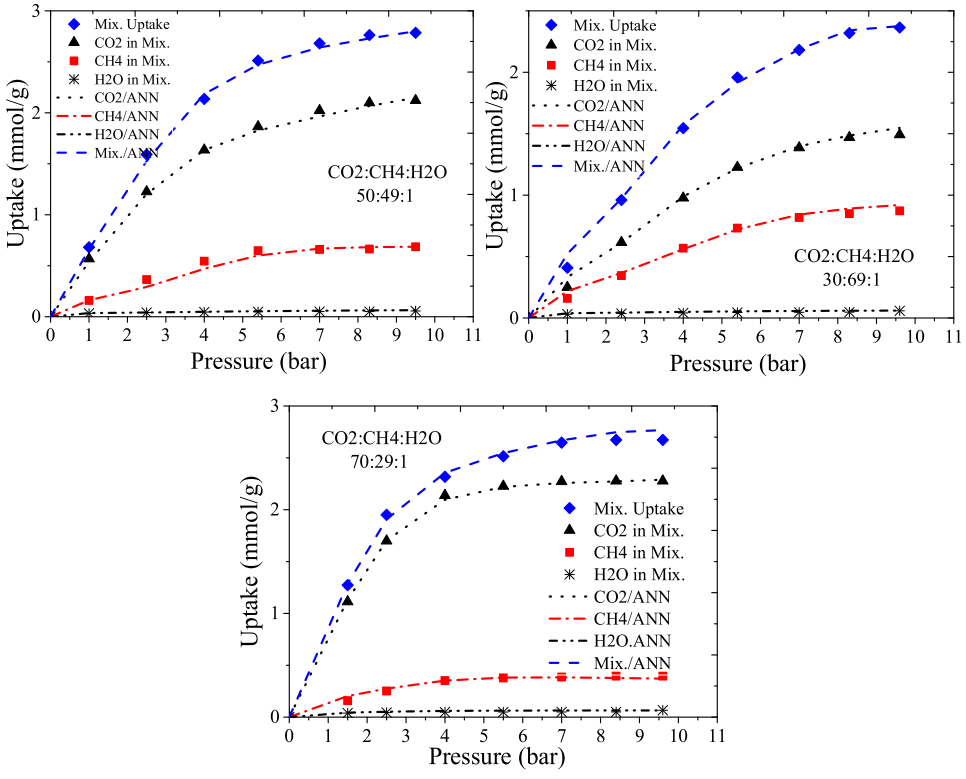

Fig. 11. Ternary CO_2:CH_4:H_2O gaseous–vapor total mixtures and partial uptakes on 5A zeolite at experimental condition of 70 °C and pressure of up to 10 bar.

Table 5
Ternary CO_2:CH_4:H_2O mixtures total and partial uptakes on 5A MSZ.

Uptakes at 50 °C (mmol/g)			
Configuration	30:69:1	50:49:1	70:29:1
Total mixture	2.803	3.129	3.214
CO_2	1.724	2.351	2.713
CH_4	1.101	0.756	0.500
H_2O	0.057	0.054	0.054
Uptakes at 70 °C (mmol/g)			
Configuration	30:69:1	50:49:1	70:29:1
Total mixture	2.364	2.784	2.672
CO_2	1.492	2.121	2.277
CH_4	0.872	0.686	0.395
H_2O	0.058	0.056	0.066

for separation and purification knowledge recently existed [63–66] in the coming future investigations. However, ANN model was developed and used to predict the combinations at the same compositions and operational conditions. The predicted data showed high agreement and certainty linked with the experimental data selected. This encouraged the simulation of further combinations and compositions to be studied and analyzed, which will be illustrated in the next section, to observe the artificial intelligence reliability in term of multicomponent mixtures and applications.

The selective isotherms indicated that CO_2 gas had the preference to be adsorbed first by 5A zeolite, even with the competitiveness between the three adsorbates considered. Water vapor experienced the lowest uptake of the mixture, and water vapor existence reduced the total adsorption uptake for the other components. This trend is clearly demonstrated by comparing the ternary mixtures results with the gaseous binary without water vapor existence as shown in Figs. 9 and 10. Table 5 presents the gravimetric total uptake of the ternary mixtures CO_2:CH_4:H_2O at three various configurations (50:49:1; 30:69:1; and 70:29:1). In addition, individual uptakes for each component as dependent isotherms have been illustrated separately. From the data presented it can be visibly observed how individual uptakes of CO_2 and CH_4 affected by initial compositions of the ternary mixtures studied. CO_2 showed high adsorption uptake even with low initial loading as in the case of 30:69:1, and how the total uptake reduced with the decrease of initial CO_2 loading. In the case of 70% CO_2, the amount of CO_2 adsorbed showed high uptake compared to the other situations.

It can be observed from the ternary mixtures results that more CO_2 percentage directs to higher uptake recorded for the total mixture uptake, which connected the proportional relation between CO_2 existence and total uptake for the mixture. With a higher concentration of CO_2 in the ternary mixture also revealed that water vapor adsorption was promoted at the same time. From the ternary (i.e.: 70% CO_2) and binary mixtures (i.e.: 99% CO_2) the water vapor adsorption showed higher values whenever CO_2 was mixed in higher compositions.

However, in the case of 50 °C binary (99:1 CO_2:H_2O) mixture, lower values of water vapor adsorption capacity was observed compared to ternary 70%CO_2: 29%CH_4: 1% H_2O mixtures adsorption and the same trend was observed in the case of 70 °C. This might refer to a longer period for ternary experiments (around 72 h) equated to faster CO_2:H_2O experiment period (around 48 h). Zeolites tend to have high adsorption capacity to water vapor with the very long period for overload accomplishments. Zeolites have more attraction to adsorb humidity compared to silica gel or clay. This was reflected by the high heat of adsorption for water on zeolites matched to the other solid desiccants [67].

Binary gas mixtures with preloaded water vapor

For this study, the 5A zeolite was pre-saturated with water vapors, with the same percentage of water presented to the adsorbents at ternary mixture measurements. Gas mixtures of CO_2 and CH_4 were premixed and dosed to the zeolite at the same composition and conditions as utilized in the binary gas mixtures, to study the difference in adsorption performance between binary gaseous mixtures, the pre-mixed ternary mixtures of CO_2:CH_4:H_2O, and CO_2:CH_4 adsorbed on zeolites preloaded with water. Figs. 12 and 13 present the difference of binary gaseous mixtures CO_2:CH_4 with the existence of preloaded water vapor at different configurations. On top of that, the ANN model was applied to predict the mixtures. The predicted data showed high agreement with the experimental data tested. Further simulated combinations were studied and analyzed, which will give better vision on the possibility to apply artificial intelligence for such technical applications and kind of data.

As shown in Table 6, at CO_2:CH_4 mixture of 50:50, the overall adsorption uptake in the case of 50 °C was slightly reduced from 3.129 mmol/g for the ternary mixture, as shown in Table 5, to 3.112 mmol/g when 1% of water vapor was preloaded in the zeolite. CO_2 and CH_4 individual adsorption within the mixture also slightly dropped from 2.351 mmol/g and 0.756 mmol/g, respectively in ternary mixtures to 2.325 mmol/g and 0.743 mmol/g in preloaded water vapor measurements. The same trend is observed in the case of 70 °C as well, with lower values of total and partial components uptakes in preloaded water vapor zeolites and this observation was consistent for CO_2:CH_4 mixtures at 30:70 and 70:30 ratios.

This can be referred to the water vapor invasion of the deep pores and cavities of the adsorbent, which will be less vacant to accommodate other adsorbents such as CO_2 or CH_4. Moreover, the reduction was highly noticeable if compared to the binary gaseous measurements without water presence at same conditions. In the 30:70 mixing ratio of CO_2:$CH_4$and 50 °C condition, the overall uptake of the mixture was reduced from 2.803 mmol/g in ternary mixture to 2.802 mmol/g with preloaded water vapor, while the individual CO_2 and CH_4 adsorption reduced from 1.724, and 1.101 mmol/g in ternary mixture to 1.718, 1.086 mmol/g in the preloaded water vapor mixtures. In the case of 70:30 mixing ratio of CO_2, CH_4, the total mixture reduced from 3.214 mmol/g to less than 3.193 mmol/g with preloaded water vapor mixture, while CO_2 and CH_4 selective individual components uptake in mixture dropped from 2.713, 0.500 mmol/g in ternary mixture to 2.709, 0.499 mmol/g in preloaded water vapor mixtures, respectively.

ANN modeling and simulation

Since ANN model has the flexibility to be trained based on the assigned output, this model is used in this study to predict the more complicated multicomponent mixture environment. Fig. 14 shows the comparison between experimental and ANN model predicted data for ternary mixture at the studied conditions i.e. 50 °C and 70 °C and pressure up to 10 bar pressures on 5A MSZ. The values of R^2 for the fitted data comparison between experimental and ANN model predicted data is shown in Fig. 14. From the values of the R^2 along with AAD% i.e. 1.03–1.79, it can be perceived that the predicted data by ANN model were highly fitted and in good agreement with the experimental results, and thus can be further processed to simulate other formations and compositions of multicomponent mixtures.

According to the consistent experimental incline increment of the total mixture with CO_2 increase percentage in the mixture, and the reversed proportion with CH_4 on the both studied thermal conditions. Where the X-axis represented the y_{CO_2} in the mixture,

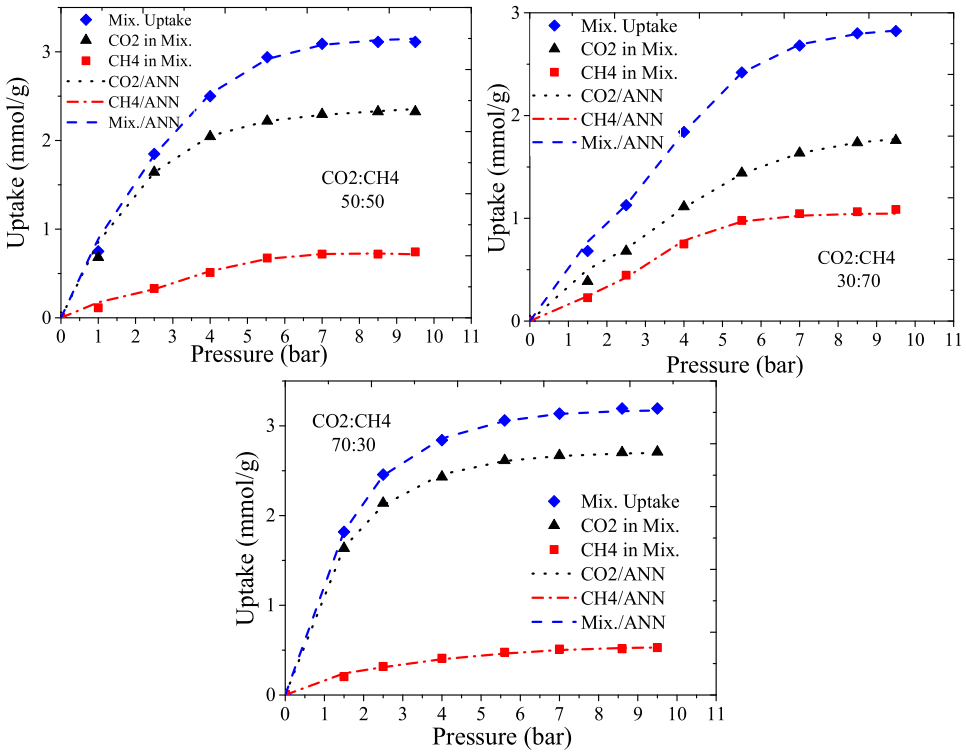

Fig. 12. Binary CO_2:CH_4 gaseous mixtures with pre-saturated water vapor on 5A zeolite at temperature of 50 °C and pressure up to 10 bar.

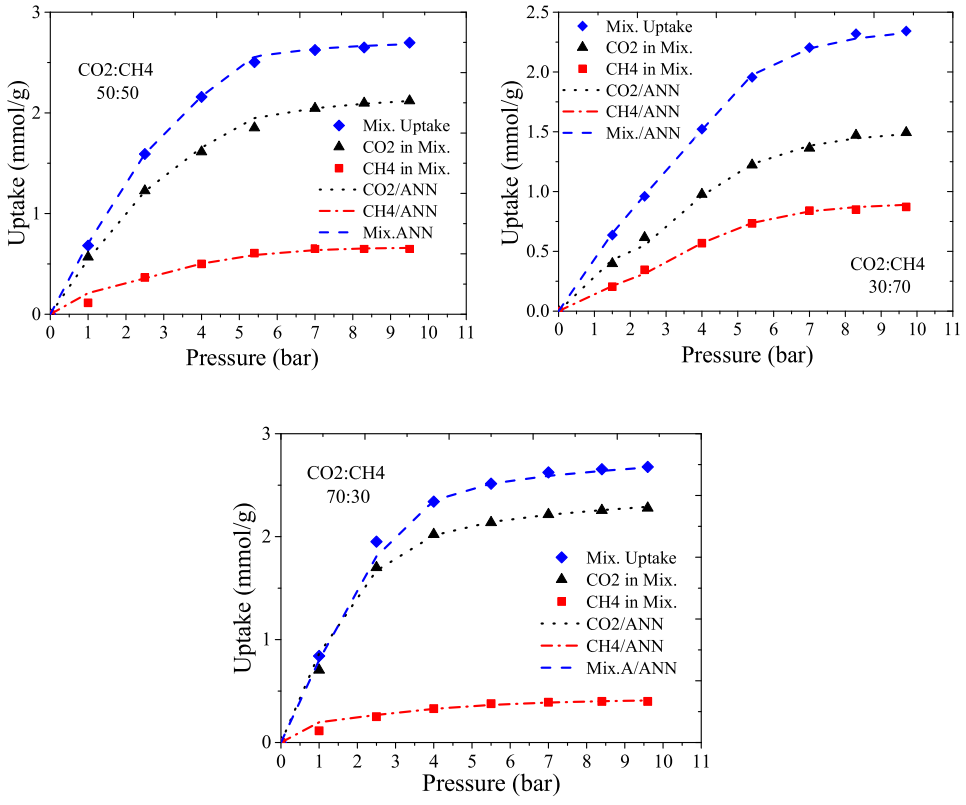

Fig. 13. Experimental binary CO_2:CH_4 gaseous mixtures with the pre-saturated water vapor on 5A MSZ at temperature of 70 °C and pressure up to 10 bar.

Table 6
Binary gaseous CO_2:CH_4 mixture total and partial adsorption uptakes for pre-saturated 5A zeolite samples with water vapor.

Uptakes at 50 °C (mmol/g)			
Configuration	30:70	50:50	70:30
Total mixture	2.802	3.112	3.193
CO_2	1.718	2.325	2.709
CH_4	1.086	0.743	0.499
Uptakes at 70 °C (mmol/g)			
Configuration	30:70	50:50	70:30
Total mixture	2.342	2.697	2.677
CO_2	1.493	2.120	2.278
CH_4	0.871	0.652	0.399

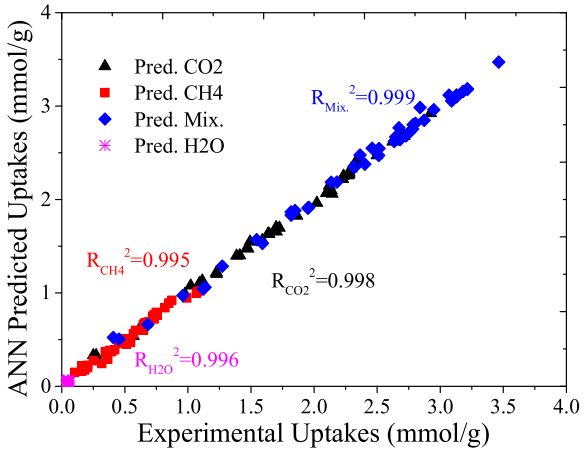

Fig. 14. Comparison between experimental and ANN model predicted uptakes data for ternary mixtures on 5A MSZ.

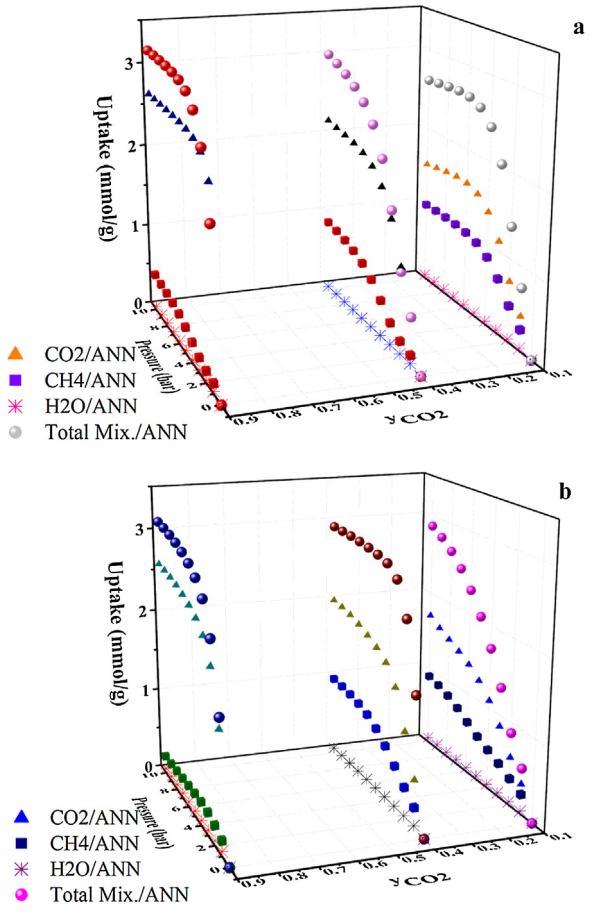

Fig. 15. Simulated total and partial uptakes of ternary CO_2:CH_4:H_2O mixtures on 5A MSZ using ANN model at pressure of up to 10 bar and temperature of (a) 50 °C and (b) 70 °C.

the Y-axis expressed the pressure and the Z-axis demonstrated the total and partial components uptakes at that particular composition. Similarly, for water vapor, the data showed the increased water uptake with CO_2 increased composition in the mixture for the experimental (i.e. 30, 50, and 70% y_{CO_2}) and simulated via ANN model (10, 40, and 90% y_{CO2}) outlined data as illustrated in Fig. 15. The consistent results may deliver a highlighted point of view for separation of natural gas that leads to more informative and innovative studies linked to selective separation of undesired components within the mixture combinations.

Fig. 16 shows the comparison between experimental and ANN model predicted data for binary gaseous with pre-saturated water vapor mixtures at the studied conditions i.e. 50 °C and 70 °C and pressure up to 10 bar pressures on 5A MSZ. The values of R^2 for the fitted data comparison between experimental and ANN model predicted data is shown in Fig. 16. The predicted data by ANN model was also highly fitted and in good agreement with the experimental results for pre-saturated water vapor condition.

Fig. 17 was illustrated the composition variation effect of the six (6) configurations (i.e. simulated by ANN) on both studied temperatures. In the figures, the outlined data showed an obvious difference in CO_2 and CH_4 partial uptakes compared to the total mixture uptake. The drop on all configurations can be observed after an increase in adsorption temperature. However, the simulated data showed good consistency to the experimental data related to the total and partial uptakes in terms of composition and temperature effects in the studied pressure range.

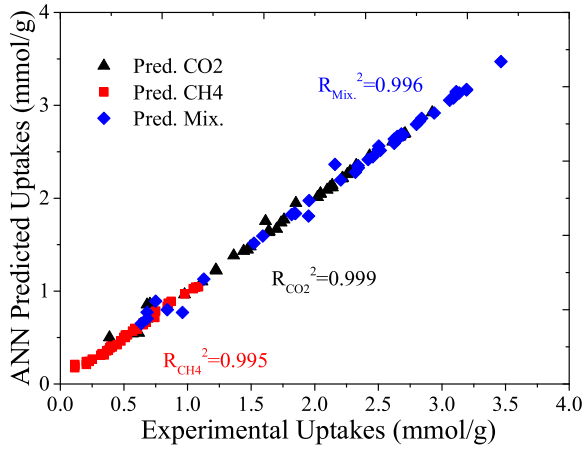

Fig. 16. Comparison between experimental and ANN model predicted uptakes data for binary gaseous with pre-saturated water vapor mixtures on 5A MSZ.

These results signify that preloaded water vapor reduces the adsorption capacity and selectivity as a greater competitive compared to the equal opportunity to ternary mixtures components. This observation is consistent with findings by Billemont et al. [68] who studied for adsorption for pure CO_2 and CH_4 on pre-adsorbed water samples, as water existence impact on adsorptions. The findings of their study indicated that the pore-filling

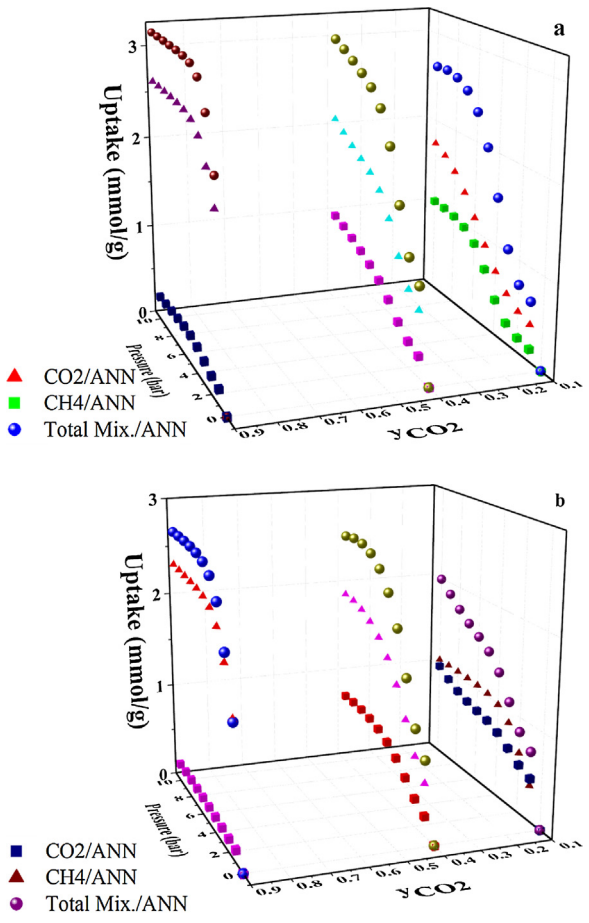

Fig. 17. Simulated binary gaseous CO_2:CH_4 Mixtures with pre-loaded water vapor using ANN model on 5A MSZ at (a) 323 K and (b) 343 K and 10 bar.

mechanism did not show highly liability by water existence and the adsorbed amount of methane or carbon dioxide declined linearly with the value of water preloaded, which agreed with the outcomes of this work, with a further extension for multi-component systems analysis.

Conclusion

In this work, a newly developed volumetric-gravimetric system with implemented GERG2008 Eos was utilized to measure CO_2:CH_4:H_2O selective adsorption for every single component in the gas–vapor mixture. Binary and ternary measurements revealed that the entire isotherm followed the same trend as the highest component percentage, while the higher CO_2 percentage led towards higher total uptake of the mixture. Correspondingly water vapor existence noticed to be reduced the total mixture uptake, in addition to the reduction of individual components uptakes. However, further reduction effect was observed with the preloaded water vapor compared to premixed ternary combinations. CO_2 and CH_4 showed lower uptake in single gas–vapor mixtures compared to pure adsorption, for instance, ≈4.05 mmol/g compared to 1.23 mmol/g for CH_4 at 50 °C. Therefore, the existence of water vapor can exert a negative influence on capacity and selectivity of solid adsorbent studied. ANN model predicted data showed high agreement with the experimental ternary measurements with high R^2 and concise low AAD% values ≈1.03–1.79. Also, the simulated combinations showed high consistency to experimental data and temperatures difference, compared to EL and MEL.

Acknowledgments

The financial and technical support from CO_2 Research Center (CO2RES), Chemical Engineering Department, Universiti Teknologi PETRONAS, Malaysia is gratefully acknowledged.

References

[1] N. Linares, A.M. Silvestre-Albero, E. Serrano, J. Silvestre-Albero, J. Garcia-Martinez, Chem. Soc. Rev. 43 (2014) 7681.
[2] M.-M. Titirici, R.J. White, N. Brun, V.L. Budarin, D.S. Su, F. del Monte, J.H. Clark, M.J. MacLachlan, Chem. Soc. Rev. 44 (2015) 250.
[3] M.E. Boot-Handford, J.C. Abanades, E.J. Anthony, M.J. Blunt, S. Brandani, N. Mac Dowell, J.R. Fernandez, M.-C. Ferrari, R. Gross, J.P. Hallett, R.S. Haszeldine, P. Heptonstall, A. Lyngfelt, Z. Makuch, E. Mangano, R.T.J. Porter, M. Pourkashanian, G.T. Rochelle, N. Shah, J.G. Yao, P.S. Fennell, Energy Environ. Sci. 7 (2014) 130.
[4] P. Markewitz, W. Kuckshinrichs, W. Leitner, J. Linssen, P. Zapp, R. Bongartz, A. Schreiber, T.E. Muller, Energy Environ. Sci. 5 (2012) 7281.
[5] J. Wang, L. Huang, R. Yang, Z. Zhang, J. Wu, Y. Gao, Q. Wang, D. O'Hare, Z. Zhong, Energy Environ. Sci. 7 (2014) 3478.
[6] K.S. Knaebel, Adsorbent, Selection. Adsorption Research, Inc., Dublin, Ohio (2004) 43016.
[7] N.H. Darman, A.R. Harun, The petroleum policy and management (PPM) project, 4th Workshop of the China-Sichuan Basin Study, Beijing, China, 2006.
[8] J.K. Adewole, A.L. Ahmad, S. Ismail, C.P. Leo, Int. J. Greenh. Gas Control 17 (2013) 46.
[9] A. Alonso-Vicario, J.R. Ochoa-Gómez, S. Gil-Río, O. Gómez-Jiménez-Aberasturi, C.A. Ramírez-López, J. Torrecilla-Soria, A. Domínguez, Microporous Mesoporous Mater. 134 (2010) 100.
[10] O. Cheung, N. Hedin, RSC Adv. 4 (2014) 14480.
[11] S. Ullah, M.A. Bustam, A.M. Shariff, A.E.I. Elkhalifah, G. Murshid, N. Riaz, AIP Conference Proceedings 1621 (2014) 34.
[12] J.M. Míguez, J.M. Garrido, F.J. Blas, H. Segura, A. Mejía, M.M. Piñeiro, J. Phys. Chem. C 118 (2014) 24504.
[13] M.A. Monsalvo, A.A. Shapiro, Fluid Phase Equilib. 254 (2007) 91.
[14] S. Ottiger, R. Pini, G. Storti, M. Mazzotti, Langmuir: ACS J. Surf. Colloids 24 (2008) 9531.
[15] A. Austegard, E. Solbraa, G. De Koeijer, M.J. Mølnvik, Chem. Eng. Res. Des. 84 (2006) 781.
[16] H.A.A. Farag, M.M. Ezzat, H. Amer, A.W. Nashed, Alexandria Eng. J. 50 (2011) 431.
[17] G.D. Pirngruber, L. Hamon, S. Bourrelly, P.L. Llewellyn, E. Lenoir, V. Guillerm, C. Serre, T. Devic, ChemSusChem 5 (2012) 762.
[18] A.A. Olajire, Energy 35 (2010) 2610.
[19] Renjith S. Pillai, Sunil A. Peter, R.V. Jasra, Microporous Mesoporous Mater. 113 (2008) 268.
[20] J. Ethiraj, F. Bonino, J.G. Vitillo, K.A. Lomachenko, C. Lamberti, H. Reinsch, K.P. Lillerud, S. Bordiga, ChemSusChem 9 (2016) 713.
[21] D.-L. Chen, H. Shang, W. Zhu, R. Krishna, Chem. Eng. Sci. 117 (2014) 407.
[22] R. Krishna, J.M. van Baten, J. Membr. Sci. 383 (2011) 289.
[23] A. Ladshaw, S. Yiacoumi, C. Tsouris, D. DePaoli, Fluid Phase Equilib. 388 (2015) 169.
[24] Y. Shen, J. Bai, Chem. Commun. (Camb.) 46 (2010) 1308.
[25] S. Ullah, A.M. Shariff, M.A. Bustam, A.E.I. Elkhalifah, G. Gonfa, F.A.A. Kareem, J. Chin. Chem. Soc. 63 (2016) 1022.
[26] S.-Y. Lee, S.-J. Park, J. Ind. Eng. Chem. 23 (2015) 1.
[27] D.W. Lee, B.R. Yoo, J. Ind. Eng. Chem. 38 (2016) 1.
[28] S. Ullah, A.M. Shariff, M.A. Bustam, A.E. Elkhalifah, G. Murshid, N. Riaz, B. Shimekit, Appl. Mech. Mater. 625 (2014) 870.
[29] S. Brull, V. Pavan, J. Schneider, Eur. J. Mech.: B/Fluids 33 (2012) 74.
[30] L. Hamon, N. Heymans, P.L. Llewellyn, V. Guillerm, A. Ghoufi, S. Vaesen, G. Maurin, C. Serre, G. De Weireld, G.D. Pirngruber, Dalton Trans. 41 (2012) 4052.
[31] A.R. Noorpoor, S. Nazari Kudahi, J. Environ. Chem. Eng. 4 (2016) 1081.
[32] M. Nematollahi, A. Jalali-Arani, K. Golzar, Appl. Clay Sci. 97 (2014) 187.
[33] K. Golzar, S. Amjad-Iranagh, H. Modarress, Measurement 46 (2013) 4206.
[34] K. Golzar, S. Amjad-Iranagh, H. Modarress, J. Dispers. Sci. Technol. 35 (2014) 1809.
[35] H. Karimi, F. Yousefi, Chin. J. Chem. Eng. 15 (2007) 765.
[36] F. Fotoohi, S. Amjad-Iranagh, K. Golzar, H. Modarress, Phys. Chem. Liquids 54 (2016) 281.
[37] F.A. Abdul Kareem, A.M. Shariff, S. Ullah, L.K. Keong, N. Mellon, Microporous Mesoporous Mater. 258 (2018) 95.
[38] F.A. Abdul Kareem, A.M. Shariff, S. Ullah, F. Dreisbach, L.K. Keong, N. Mellon, S. Garg, J. Nat. Gas Sci. Eng. 50 (2018) 115.
[39] A. Rana, A. Patra, M. Annamalai, A. Srivastava, S. Ghosh, K. Stoerzinger, Y.-L. Lee, S. Prakash, R.Y. Jueyuan, P.S. Goohpattader, N. Satyanarayana, K. Gopinadhan, M.M. Dykas, K. Poddar, S. Saha, T. Sarkar, B. Kumar, C.S. Bhatia, L. Giordano, Y. Shao-Horn, T. Venkatesan, Nanoscale 8 (2016) 15597.
[40] R. Kumar, B. Chowdhury, Ind. Eng. Chem. Res. 53 (2014) 16587.
[41] S. Ye, J. Sun, X. Yi, Y. Wang, Q. Zhang, Sci. Rep. 7 (2017).
[42] S. Biswas, J. Zhang, Z. Li, Y.Y. Liu, M. Grzywa, L. Sun, D. Volkmer, P. Van Der Voort, Dalton Trans. 42 (2013) 4730.

[43] P. Chowdhury, S. Mekala, F. Dreisbach, S. Gumma, Microporous Mesoporous Mater. 152 (2012) 246.
[44] L. Li, J. Yang, J. Li, Y. Chen, J. Li, CrystEngComm 15 (2013) 6782.
[45] F. Dreisbach, H.W. Lösch, J. Therm. Anal. Calorim. 62 (2000) 515.
[46] F. Dreisbach, H. Lösch, P. Harting, Adsorption 8 (2002) 95.
[47] J. Moellmer, A. Moeller, F. Dreisbach, R. Glaeser, R. Staudt, Microporous Mesoporous Mater. 138 (2011) 140.
[48] L. Hamon, L. Chenoy, G. De Weireld, Adsorption 20 (2014) 397.
[49] S. Tedds, A. Walton, D.P. Broom, D. Book, Faraday Discuss. 151 (2011) 75.
[50] F.A. AbdulKareem, A.M. Shariff, S. Ullah, S. Garg, F. Dreisbach, L.K. Keong, N. Mellon, Energy Technol. 5 (2017) 1373.
[51] O. Kunz, W. Wagner, J. Chem. Eng. Data 57 (2012) 3032.
[52] A. Kurniawan, H. Sutiono, N. Indraswati, S. Ismadji, Chem. Eng. J. 189 (2012) 264.
[53] K. Foo, B. Hameed, Chem. Eng. J. 156 (2010) 2.
[54] S. Chakraborty, J.K. Basu, S. De, S. DasGupta, Ind. Eng. Chem. Res. 45 (2006) 4732.
[55] Y. Abdollahi, N.A. Sairi, M.K. Aroua, H.R.F. Masoumi, H. Jahangirian, Y. Alias, J. Ind. Eng. Chem. 25 (2015) 168.
[56] M. Mofarahi, F. Gholipour, Microporous Mesoporous Mater. 200 (2014) 1.
[57] J.A. Delgado, V.I. Águeda, M.A. Uguina, J.L. Sotelo, P. Brea, C.A. Grande, Ind. Eng. Chem. Res. 53 (2014) 15414.
[58] Z.R. Herm, R. Krishna, J.R. Long, Microporous Mesoporous Mater. 151 (2012) 481.
[59] P.J.E. Harlick, F.H. Tezel, Sep. Purif. Technol. 33 (2003) 199.
[60] D.L. Bish, H.-W. Wang, Philos. Mag. 90 (2010) 2425.
[61] Y. Wang, M.D. LeVan, J. Chem. Eng. Data 55 (2010) 3189.
[62] G. Li, P. Xiao, P. Webley, Langmuir: ACS J. Surf. Colloids 25 (2009) 10666.
[63] N. Heymans, B. Alban, S. Moreau, G. De Weireld, Chem. Eng. Sci. 66 (2011) 3850.
[64] B. Alp, M. Gönen, S.A. Savrık, D. Balköse, S. Ülkü, Drying Technol. 30 (2012) 1610.
[65] M.G. He, Y. Liu, N. Xin, Y. Zhang, X.J. Liu, J. Chem. Eng. Data 61 (1) (2015) 12–18.
[66] J. Rother, T. Fieback, Adsorption 19 (2013) 1065.
[67] M.S. Yeganeh, B.S. Minhas, T.I. Mizan, Z. Sufang, R.W. Flynn, Method of protecting a solid adsorbent and a protected solid adsorbent, Google Patents (2014).
[68] P. Billemont, B. Coasne, G. De Weireld, Langmuir: ACS J. Surf. Colloids 27 (2011) 1015.